Polymerization of Acrylamide in the Presence of Tetradecyltrimethylammonium Bromide Surfactant

Mukundan Chakrapani,[†,§] Randolph L. Rill,[‡] and David H. Van Winkle*[,†]

Center for Materials Research and Technology and Department of Physics, Department of Chemistry and Biochemistry, and Institute of Molecular Biophysics, Florida State University, Tallahassee, Florida 32306

Received June 16, 2003; Revised Manuscript Received September 5, 2003

ABSTRACT: The polymerization of acrylamide (AAm) and *N,N′*-methylenebis(acrylamide) (BIS) in the presence of high concentrations of tetradecyltrimethylammonium bromide (TTAB) results in formation of macroporous gels. Prior to polymerization, the presence of AAm monomer shifts the TTAB micelle to the columnar phase transition boundary. The combination of dynamic viscosity measurements and X-ray diffraction shows for high TTAB concentrations that during polymerization TTAB micelles are driven into nanodomains of the hexagonal−columnar phase. X-ray diffraction from lower concentration TTAB samples shows that micelles are limited to a closest separation of 10 nm, apparently due to the presence of the polyacrylamide network.

1. Introduction

Recent work has shown that hydrogels with controlled modifications of internal and surface structures can be produced using the templating effects of self-assembling surfactant systems.[1−18] These novel hydrogels exhibit properties that can be exploited for a variety of applications. For example, polyacrylamide gels with a controlled pore size distribution and high mechanical strength are good candidates for biomolecular separations using electrophoresis or gel permeation chromatography.[1,8,11] Additional templating within the pore channel system of these gels allows the generation of polymer/inorganic and other hybrid materials. The importance of such multiple replica procedures has been demonstrated in the synthesis of superparamagnetic rubbers and highly porous, continuous TiO_2 networks for photocatalytic applications.[17]

Patterson[1] performed a systematic study to find good templating candidate systems for creating gels with internal pore structures advantageous for chromatography. These novel gels would be used for targeted size separations of proteins or nucleic acids. Surfactants were dissolved in solutions of acrylamide monomers that were subsequently polymerized. The surfactants were then soaked out of the resulting gels. Gel permeation chromatography using polyacrylamide gels formed in the presence of surfactants indicated that these gels were extremely durable and had a macroporous structure. The porosities of the gels could be varied a great deal, independent of monomer or cross-linker concentrations by using the surfactant as a structure-directing agent.

Several unusual results were found when acrylamide monomer was polymerized in the presence of surfactants. In many cases, the resulting gel would be clear, but when placed in water for surfactant removal, the gel would become white. Atomic force microscopy (AFM) studies showed that surfaces of polyacrylamide gel surfaces formed in the absence of surfactant were flat and featureless, while gels formed in the presence of 40 wt % surfactant exhibited a high density of bumps ∼150 nm high.[19] The surface features revealed by AFM were analyzed by numerical scaling analysis.[20] This study showed that the long length scale features would give rise to significant light scattering, thus explaining the whiteness of gels following surfactant removal. In addition, chromatographic separations of large proteins using crushed templated gels showed that even the largest proteins were retarded in the gel, indicating the presence of large-scale pores.[1]

We report here studies of the acrylamide/surfactant system before, during, and after gelation using polarized light microscopy, X-ray diffraction, rheometry, and optical transmission measurements. The presence of acrylamide monomer changes the surfactant phase diagram: the transition from isotropic micellar to hexagonal−columnar phase moves to higher surfactant concentrations. Gelation is slowed by the presence of surfactant, and as the gel forms, surfactant ordering occurs within the polymerizing gel and in phase-separated nanoregions. For moderate surfactant concentrations, gels contain isotropically distributed micelles separated by at least 10 nm and nanoregions of the hexagonal−columnar phase. For high surfactant concentrations, upon gelation the surfactant mostly phase separates into a connected network of hexagonal−columnar domains. Upon soaking gels formed with high surfactant concentrations, all surfactant diffuses out, leaving the polyacrylamide network surrounding nanoregions now filled with only water. These appear white due to the index of refraction mismatch of water and polyacrylamide gel. In chromatography, even very large proteins (radius of gyration 6−7 nm) can explore the porous network left behind when the hexagonal−columnar surfactant domains are soaked out.

2. Experimental Section

2.1. Materials and Synthesis. Stock solutions of 40 wt % acrylamide (Electrophoresis grade, Fisher Scientific) plus

† Center for Materials Research and Technology and Department of Physics.
‡ Department of Chemistry and Biochemistry and Institute of Molecular Biophysics.
§ Current address: Steacie Institute for Molecular Sciences, National Research Council, Ottawa, ON K1A 0R6, Canada.
* Corresponding author: phone 850 644 6019; Fax 850 644 6504; e-mail rip@physics.fsu.edu.

10.1021/ma034814m CCC: $25.00
Published on Web 10/29/2003

cross-linker (*N,N′*-methylenebis(acrylamide)) (BIS) in TBE buffer (45 mM Tris-borate, 1 mM Na_2EDTA) at pH 8.3 were prepared. The concentration of the BIS with respect to acrylamide was 7 wt %. The total acrylamide concentration in the stock solution was calculated as a mass percentage, assuming a density of 1.00 g/cm^3 for water and buffer solution added; that is

$$\% T = [M_a/(M_a + M_l)] \times 100 \quad (1)$$

where M_a is the mass of acrylamide (including BIS) and M_l is the mass of solution (water plus buffer concentrate). The surfactant tetradecyltrimethylammonium bromide (TTAB, Sigma-Aldrich) was dissolved in the acrylamide stock solution to form the "pregel" solutions. Samples were made with surfactant concentrations ranging from $S = 0$ to 40 wt % of the stock solution. The surfactant concentration was calculated as

$$\% S = [M_s/(M_s + M_p)] \times 100 \quad (2)$$

where M_s is the mass of surfactant and M_p is the mass of the stock solution.

The pregel solutions were polymerized at room temperature by free-radical polymerization with chemical initiators. For every 10 mL of pregel solution, 40 μL of 10 wt % ammonium persulfate and 8 μL of *N,N,N′,N′*-tetramethylethylenediamine (TEMED, Fisher Scientific) were used to initiate polymerization. Gels were soaked in distilled water to remove the surfactants by diffusion after polymerization for about 2−4 days. More than 98% of the surfactants diffused out of the gel upon soaking for about 2 days. Several methods, including Raman spectroscopy, have been used to quantify the removal of the surfactants by free diffusion into water.[1] Specific sample preparation techniques adopted for different experiments are described under the respective sections.

2.2. Polarized Light Microscopy. The relevant portion of the phase diagram of TTAB solutions was verified by polarized optical microscopy and by rheometry. A series of solutions with TTAB concentrations ranging from 0% to 40%, in steps of 10%, were prepared in buffer and in buffered 40% acrylamide solutions. Glass capillary tubes (1.5 mm o.d., 0.01 mm thickness, and 80 mm length, Charles Supper) were filled with TTAB solutions, and the samples were examined for characteristic birefringence patterns using a Nikon Optiphot-2 polarizing microscope under a 20× objective and 10× eyepiece.

2.3. Refractive Index Measurements. Refractive index measurements were performed using a prism refractometer (Bausch and Lomb). Solutions with concentrations of 10, 20, 30, and 40% of buffered acrylamide and TTAB were prepared in glass culture tubes (Fisher Brand). Similarly, samples were made by dissolving TTAB in 40% buffered acrylamide solutions with concentrations of 0−40%, in steps of 10%. Three refractive index values were measured for each sample and averaged.

2.4. Dynamic Rheology Measurements. Small-amplitude oscillatory stress measurements were done using a commercial rheometer (Rheostress300, Thermo Haake) with a cone−plate geometry. A plate radius of 30 mm and a cone angle of 2° were used. The dynamic viscosities $|\eta^*|$ of buffered TTAB solutions with concentrations of 0, 10, 20, 22, 24, 26, 28, 30, 35, and 38% were determined. To get detailed information about the phase diagram in the presence of acrylamide, the dynamic viscosities of a series of 40% buffered acrylamide solutions with TTAB concentrations ranging from 0 to 45% in small steps were measured. The measurements were repeated three times, and data were collected for 60 s each. Real-time viscosity measurements were made after the initiation of polymerization in pregel solutions containing 0, 10, 15, 20, 22, 25, 28, 30, 38, and 40% TTAB. For real-time dynamic viscosity measurements, polymerization was initiated in 1.5 mL disposable microtubes (Fisher Brand) just prior to loading the sample onto the rheometer. A small amount of the sample was then transferred to the measuring plate. The dynamic viscosity $|\eta^*|$, storage modulus G', and loss modulus G'' were recorded as a function of polymerization time at a constant frequency of $\omega = 1$ Hz and a stress of 10 Pa. All data were collected for 10 000 s from the time of addition of the initiators. The typical time interval between the initiation of polymerization and the start of data collection was about 30 s.

2.5. X-ray Diffraction. X-ray scattering measurements were made using a 12 kW Rigaku Rotating anode generator (Rigaku RU-H2R) (Cu Kα radiation, $\lambda = 1.5418$ Å) equipped with an Osmic Blue confocal mirror system and a Rigaku image plate detector (R-Axis IIc). The tube voltage was 90 kV and the tube current 40 mA. The sample-to-detector distance was 465 mm. The data collection and processing was controlled by a dedicated Dell Precision workstation. X-ray scattering data were collected from 0, 10, 20, 30, and 40% TTAB solutions in buffer and in 40% buffered acrylamide. The solutions were drawn into glass capillary tubes (o.d. 1.5 mm, 0.01 mm thickness, and 80 mm length, Charles Supper). A similar set of capillary tubes were filled after the initiation of polymerization of 0, 10, 15, 20, 22, 25, 28, 30, and 40% pregel solutions. The tubes were immediately flame-sealed, allowing the gels to form inside the tubes. The gels were cured overnight and then used for X-ray scattering studies. Gels were also made separately in 1.5 mL disposable microtubes (Fisher Brand). These gels were soaked in 50× distilled water for 5 days in order to remove the surfactants. The water used for soaking was changed daily. The soaked gels were then crushed and placed in capillary tubes for X-ray scattering studies.

The scattering data were circularly averaged using the DISPLAY program available with the R-Axis system. The circularly averaged data were then corrected by subtracting the background data (from samples without the TTAB) from the data obtained for the samples with TTAB. That is, scattering data of a sample of pure buffer were subtracted from the data obtained for TTAB solutions in buffer, scattering data of a sample of 40% acrylamide solution were subtracted from the data obtained for TTAB solutions in acrylamide, and scattering data of a sample of 40% polyacrylamide gel formed without TTAB were subtracted from the data obtained for the gels formed in the presence of TTAB. The background subtraction required suitable scaling of the background data to match the intensities of the large scattering vector tails of the data. An automated peak fitting program (PeakFitv4.0, Jandel Scientific) was used to identify the locations of peaks by the deconvolution method using a Voigt function model.[21]

2.6. Optical Transmission Measurements. The optical transmission of the gels was measured using a laser source and photodiode detector. Light from a He−Ne laser (4 mW, Uniphase Inc., San Jose, CA) was directed from above a watch glass used as a sample holder and onto a photodiode (Thor Labs) placed below the holder. The output voltage of the photodiode was measured with a digital multimeter (Radio Shack).

Gels were formed in the presence of 0, 10, 20, 25, 28, 30 and 40% TTAB between glass slides as described in ref 19. The gels were peeled off the glass slide and immediately placed in the sample holder filled with distilled water. The voltage as displayed on the multimeter was recorded by hand every 30 s for 10 min. For gels formed in the presence of 30% TTAB, data were recorded in 30 s intervals for up to 30 min and subsequently in 5 min intervals (if needed). The transmittance of the various gels was calculated by dividing the voltage output of the photodiode with gel present by the voltage output of the photodiode without the gel present in the holder.

3. Results

3.1. Pregel Solutions. The final structure formed after polymerization of acrylamide and removal of surfactant is based in part on the structures formed before polymerization. The pregel solution consists of acrylamide monomer in buffer and TTAB molecules that are known to self-associate into micelles. Changes in the acrylamide monomer behavior due to the presence of TTAB are difficult to quantify. For example, one

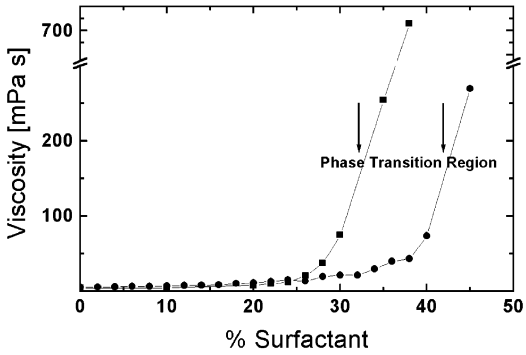

Figure 1. Viscosity of different TTAB concentrations in buffer and in acrylamide solutions. The transition region where the isotropic micellar solution becomes anisotropic occurs at about 35% in buffer solution but is shifted to about 45% in the acrylamide solution.

might imagine that the hydration of the acrylamide monomers might be affected by the presence of a high concentration of surfactant molecules. We know of no signature experiment to reveal changes in hydration directly. On the other hand, if the TTAB structure changed, that might be revealed in polarized microscopy, changes in viscosity, and structural features probed by X-ray diffraction. Several concentrations of TTAB in buffered 40% acrylamide stock solution were studied to discover these changes.

Polarized light microscopy of TTAB in buffer solutions up to 30 wt % revealed no birefringence, suggesting an isotropic micellar solution. Characteristic birefringence patterns consistent with a hexagonal−columnar phase were observed when the TTAB concentration was increased to 40%. By contrast, no birefringence was observed in buffered acrylamide solution with TTAB concentration up to 40%. Birefringence was seen, however, when the TTAB concentration was increased to 45%.

The viscosities of TTAB in buffer and of TTAB in acrylamide stock solution are shown as a function of TTAB concentration in Figure 1. Both sets of data show a relatively small rise in viscosity with increasing TTAB concentration followed by a more significant increase. Without TTAB the viscosity of the buffer solution was 3.8 mPa s, and the acrylamide stock solution's was 5.0 mPa s, consistent with a higher viscosity for the solution with more dissolved solids. This pattern persists with increasing TTAB concentration until the viscosity of the TTAB in buffer becomes larger than the TTAB in acrylamide at 26% TTAB. For higher TTAB in buffer concentrations the viscosity increases dramatically. A similar dramatic increase in viscosity of the TTAB in acrylamide solution occurs for TTAB concentrations about 10% higher than for TTAB in buffer. In both cases, the dramatic increase in viscosity likely signals an increase in intermicellar interactions as the isotropic micellar solution becomes anisotropic.[22] Thus, these data suggest the presence of acrylamide suppresses the intermicellar interactions, such that similar effects require significantly higher surfactant concentrations.

Small-angle X-ray scattering data from solutions of TTAB in buffer and in acrylamide were obtained with an "image plate" area detector in the beam path. Plots of circularly averaged X-ray scattering intensity $I(q)$, corrected for background, are shown in Figure 2. The circularly averaged plots were fit with Voigt functions, and the length scales associated with the dominant peak centers are summarized in Table 1. The 10 wt % TTAB in buffer solution produced two diffuse scattering peaks at $q = 0.09$ Å^{-1} and $q = 0.137$ Å^{-1} (Figure 2a). The q values ($q = (4\pi \sin \theta)/\lambda$, where 2θ is the angle between incident and scattered radiation) correspond to mean Bragg distances of $d = 7.1$ and 4.6 nm ($d = \lambda/(2 \sin \theta)$). Following Itri and Amaral,[23] the first peak (in increasing q) is attributed to the structure factor or the intermicellar interference term. The associated length scale ($d = 7.1$ nm) then corresponds to the average spacing between micelles within the scattering volume. The second peak ($d = 4.6$ nm) is attributed to the form factor, which in this case is the effective micelle diameter, and

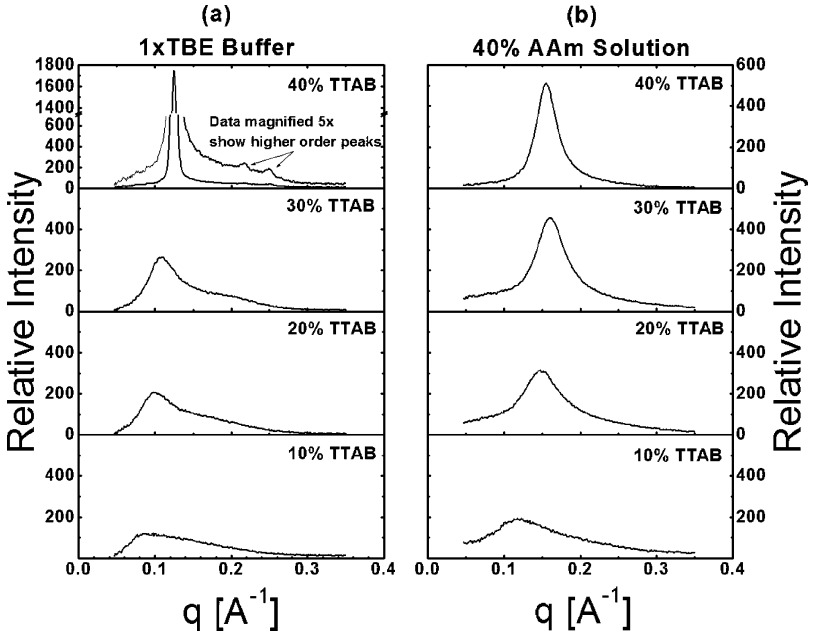

Figure 2. X-ray scattering data of various concentrations of TTAB in (a) buffer and (b) acrylamide solutions. Two peaks corresponding to intermicellar spacing and micellar dimensions are seen for all TTAB concentrations (except 40%) in buffer. The 40% TTAB in buffer solution shows a typical liquid crystalline scattering pattern corresponding to an hexagonal columnar phase. However, in the presence of acrylamide monomers, TTAB exists in the isotropic micellar phase for all concentrations studied.

Table 1. Summary of Results from Fits to X-ray Scattering Data for TTAB in Buffer and in 40% Buffered Acrylamide Solutions

	TTAB in TBE buffer		TTAB in acrylamide solution
% surfactant	peak 1 [nm]	peak 2 [nm]	peak 1 [nm]
10	7.1	4.6	4.5
20	6.3	4.2	4.2
30	5.8	3.9	4.0
40	5.0[a]	2.8[b]	4.1

[a] Characteristic [1,0] peak of a hexagonal−columnar system. [b] Characteristic [1,1] peak of a hexagonal−columnar system.

corresponds with the expected diameter of 4.2 nm for TTAB micelles[24] within the uncertainty in the fit. (The peaks are rather broad, and their absolute positions change slightly with subtle changes in background subtraction.)

For higher TTAB concentration, the peak centers shifted to larger q, corresponding to smaller length scales. The increase in q (decrease in d) of the first peak is a direct result of the increase in surfactant concentration and consequent decrease in the intermicellar spacing. The peak associated with the micellar diameter is still rather poorly defined, but the length scale associated with its center is closer to the expected 4.2 nm diameter. At higher concentrations, spherical micelles tend to become prolate ellipsoids.[23] The scattering from 40 wt % TTAB solution in buffer was highly anisotropic and characteristic of an hexagonal columnar system with a narrow primary peak at 5 nm corresponding to the nearest-neighbor distance in the [10] direction. Well-defined higher-order peaks corresponding to [11] and [20] directions were clearly observed as well (uppermost data in Figure 2a).

Circular average plots of $I(q)$ for the pregel solutions containing acrylamide and TTAB are shown in Figure 2b. There are noticeable differences in these data compared with those obtained for TTAB buffer solutions. For each TTAB concentration in AAm solutions, the signal is dominated by a peak that sits on one or more broad background peaks. The strong peak in each sample was centered at higher q with increasing TTAB concentration. The intensity of the dominant peak increased with increasing TTAB concentration as well. The scattered intensity at corresponding TTAB concentrations was higher in the presence of acrylamide than in buffer. Scattering from the 40 wt % TTAB/AAm solution was isotropic and not characteristic of a liquid crystalline system. The presence of acrylamide monomers apparently does not prevent the formation of micelles, but the transition from isotropic micellar phase to hexagonal columnar phase is affected. (In AAm solutions the columnar phase of TTAB was not observed.)

3.2. Gelation. Real-time rheological measurements are an excellent tool to study the formation of gels in the presence of surfactants. The dynamic viscosity $|\eta^*|$, storage modulus G', and loss modulus G'' were recorded as functions of polymerization time for buffered 40% acrylamide solutions with several TTAB concentrations. Figure 3 shows $|\eta^*|$ for five of these concentrations. In this plot negative times are before the gel point. In all cases, $|\eta^*|$ is constant or slowly increasing for some time following initiation of polymerization. This is called the "induction stage". Then, $|\eta^*|$ increases dramatically (by more than 5 orders of magnitude), signifying formation of a cross-linked gel spanning the gap between the cone and the plate of the viscometer. Following gelation, $|\eta^*|$ continues to increase a bit more before attaining a steady value. Norisuye et al.[25] observed a similar time evolution of scattered light intensity during the polymerization of *N*-isopropylacrylamide. For the gels formed here, the scattered light intensity does not diverge; the gels remain optically clear.

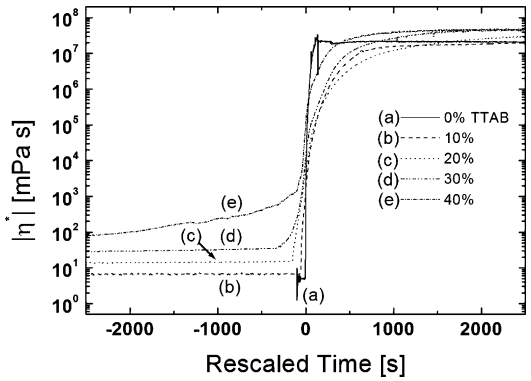

Figure 3. Dynamic viscosity measurements as a function of rescaled time in order to compare gelation behavior of the gels formed in the presence of different concentrations of TTAB. Note that, for TTAB concentrations of higher than 30%, the dynamic viscosity values show a steady rise before the onset of gelation indicating phase separation.

Polyacrylamide gel formed without any surfactant in the pregel solution, polymerized rapidly. The induction stage for these gels lasted for about 100 s. The presence of TTAB at concentrations of 10% and higher in the pregel solution slowed the polymerization considerably. In all cases the induction stage was greater than 35 min, but a clear relation between the concentration of TTAB in the pregel solution and the duration of the induction time could not be made.

For fluids, the viscoelastic response is primarily a frictional−thermal loss; hence, the loss modulus G'' dominates. For solids, the oscillations are propagated through the material, and hence the storage modulus G' dominates. To study the effect of the presence of the surfactants on gelation, we define the gel point to be $G'' = G'$.[26] This allows us to rescale the data in time consistently, to compare gelation data of different concentrations. Winter et al. showed that a proper determination of the gel point is only acquired by measuring $\tan(\delta) = G''/G'$ at different frequencies. We measured the complex viscosity at a single frequency in order to develop an understanding of the molecular level rearrangements of acrylamide and TTAB when they form a complex system. The information acquired, particularly the slow pretransitional increase in viscosity of the 30% and 40% gels to values comparable to those seen in the buffer and acrylamide solutions, gives us useful information. A more detailed measurement of the complex viscosity as a function of frequency would not likely provide additional information about these issues. For our purposes, this simpler definition helps us gain some insight into changes in the process of gelation due to the presence of TTAB by comparing data at a single frequency for many different gels. As shown in Figure 3, the time evolution of the viscosity was rescaled by setting the time $t = 0$ at the gel point for each experiment.

The time-dependent viscosities during the induction stage relate to the viscosities of the TTAB solutions (shown in Figure 1). For TTAB concentrations up to 28%, $|\eta^*|$ remained low and nearly constant throughout

Table 2. Average Maximum Dynamic Viscosity, the Time To Attain That Maximum after the Gel Point, and the Time To Reach Half the Maximum Viscosity after the Gel Point Are Tabulated as a Function of Amount of TTAB in the Gel

% surfactant	η^*_{max} [mPa s]	t_{max} [s]	$t_{1/2}$ [s]
0	2.2×10^7	150	85
10	2.6×10^7	4800	740
15	3.0×10^7	6800	820
20	3.4×10^7	6000	1400
22	3.4×10^7	4000	820
25	4.0×10^7	3000	660
28	3.4×10^7	2800	830
30	5.0×10^7	6000	500
40	6.0×10^7	6000	600

the induction period at values very similar to those measured for TTAB in acrylamide solution. At the gel point $|\eta^*|$ increased abruptly. When the TTAB concentration was 30% and higher, $|\eta^*|$ increased gradually but substantially, prior to the gel point. The dynamic viscosities of the gelling solutions during the induction time range from 10 to 30 mPa s for TTAB solutions of 10−28%, in excellent agreement with the viscosities of the pregel solutions of similar TTAB concentrations (see Figure 1). The $|\eta^*|$ values for the gel formed in the presence of 30% TTAB rose from 30 to about 100 mPa s and for 40% TTAB rose from 80 to 800 mPa s just prior to the gel point. The initial values of $|\eta^*|$ for these concentrations of TTAB are essentially the same as the measured viscosities of TTAB in acrylamide solutions. The final values of $|\eta^*|$ (just prior to the gel point) correspond to the measured viscosities of TTAB in buffer solutions at the same TTAB concentrations. Recall that these solutions showed evidence of formation of hexagonal phase, whereas TTAB solutions in buffered acrylamide did not. The higher viscosity values suggests that there may be a demixing of the polymer gel phase from the surfactant mesophase.

3.3. The Final Gel. Measurements of the dynamic viscosity for rescaled times greater than zero show that cross-linked gels form but that the presence of TTAB changes the polymerization dynamics (Figure 3). The figure shows the increase on a logarithmic scale to show the 7 orders of magnitude jump in viscosity upon gelation for all samples. The time to gel is characterized by a rapid jump in viscosity followed by a slower gradual increase over a much longer time scale. To characterize the gelation process after the gel point, we report the average value of the final dynamic viscosity, the approximate time to reach that value, and the time to attain 50% of the final viscosity in Table 2. These data indicate that the presence of TTAB slows the gelation process considerably.

The viscoelastic properties measured at long times after the gel point indicate that the gels formed have very good mechanical strength. Figure 4 shows the storage modulus G' of the samples as a function of TTAB concentration. Even for gels made with 40% concentration of TTAB the storage modulus is extraordinarily large ($G' \sim 4 \times 10^5$ Pa), despite the high gel porosity. For polyacrylamide gels made in the absence of TTAB, the storage modulus was $G' \sim 1.4 \times 10^5$ Pa. High mechanical strength is a useful property for the application of these gels as separation matrices. Patterson[1] showed that these materials could sustain several times the maximum flow rate of commercially available gels for gel permeation chromatography.

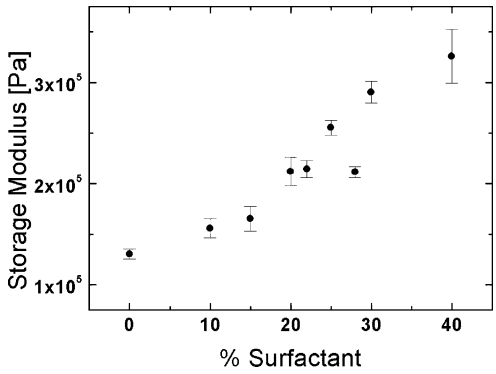

Figure 4. Storage modulus G' of gels as a function of TTAB concentration.

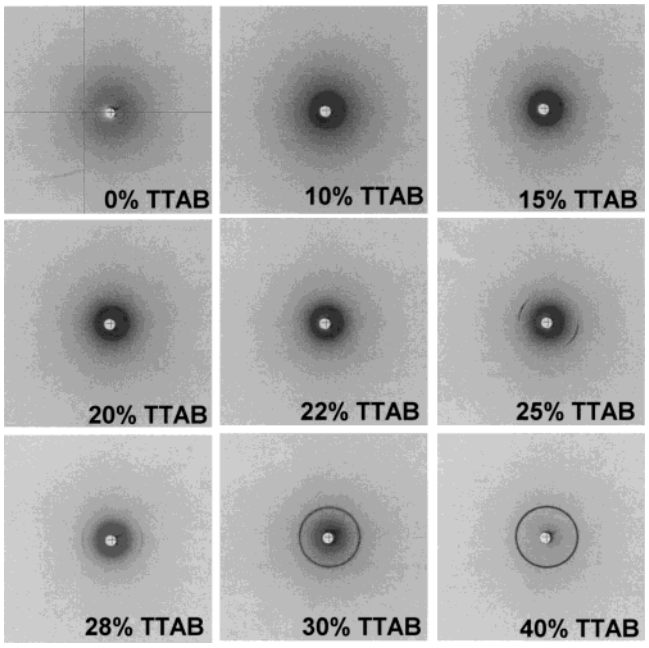

Figure 5. Two-dimensional X-ray scattering data as displayed by the image plate for various polyacrylamide gels prior to the removal of surfactant. The TTAB concentrations are indicated on each image. The bright center spot is the beam stop. Higher X-ray intensity is represented by darker pixels.

The bulk structures of the gels prior to, and after the removal of, surfactants were studied by X-ray scattering. Figure 5 shows image plate X-ray diffraction patterns for 40% polyacrylamide gels formed in the presence of TTAB surfactant at the indicated concentrations. For no added TTAB (0%) a diffuse, circularly symmetric background is observed. With increasing TTAB concentration, increasing intensity is seen near the center (white) beamstop. This intense scattering at small angles was surprising. Gels containing 25% and 28% TTAB produced arcs at higher scattering angles. The small-angle scattering remained intense. For the gel formed in the presence of 30% TTAB, the intensity of the small-angle scattering was less, and a well-defined ring was seen. In the 40% TTAB gel, the small-angle scattering was quite small, and the ring was better defined. Circular averages of these data reveal interesting details.

Plots of circularly averaged scattering intensity ($I(q)$) obtained from gels with various TTAB concentrations prior to and after the removal of the surfactant are shown in Figures 6 and 7. Figure 6 shows plots for increasing concentration from 1% to 10% TTAB. With

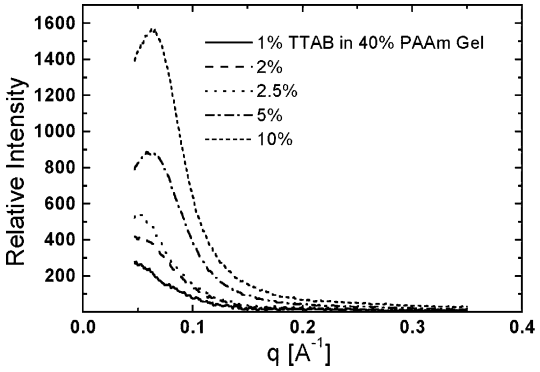

Figure 6. Circularly averaged intensity plots for TTAB concentrations in the range 1−10% prior to the removal of TTAB.

increasing concentration the small-angle peak grows in intensity and shifts to slightly higher q. The increase in intensity of small-angle scattering seems to track the TTAB concentration. Though the cutoff of the data for $q = 0.047$ Å^{-1} makes accurate comparison of fits to a single peak suspect, the increase in scattered intensity is approximately proportional to the TTAB concentration. In addition, with increasing TTAB concentration (from 2.5 to 10%) the peak's maximum increases in q, corresponding to a decrease in length scale from 12.5 to 10 nm.

In Figure 7, circularly averaged $I(q)$ are shown for 10−40% TTAB gels (solid lines) and for corresponding gels formed in the presence of TTAB, but which have been soaked to remove the surfactant (dashed lines). The large difference between the scattered intensities with and without TTAB shows that the primary signal is from the surfactant. For each TTAB concentration from 10 to 28%, there is a broad peak centered at a q corresponding to a length scale of about 10 nm. The $I(q)$ plots for gels containing 25% and 28% TTAB included a second peak with a characteristic length scale of 4 nm as well as the broad small-angle peak. Gels formed in the presence of 30% TTAB or higher yielded narrow, intense peaks centered at $q = 0.155$ Å^{-1}, corresponding to a length scale of 4 nm. In principle, the width of the peak should contain information on the size of the domains, but the beam cross section was very close to the measured width. The small-q scattering for the gels formed in the presence of 30% and 40% TTAB concentrations was less intense. The actual length scales associated with peak centers observed from gels prior to surfactant removal are presented in Table 3. The scattering profiles from all gels after surfactant removal were quite similar to each other. There was a slight enhancement in small-q scattering for all of the polyacrylamide gels, perhaps associated with the structure factor for polyacrylamide aggregates in the gels. The peaks corresponding to $d = 4$ nm that were prominent in gels containing the highest surfactant concentrations prior to soaking were not observed in gels without surfactant present.

Table 3. Summary of Results from Fits to X-ray Scattering Data for Gels before the Removal of TTAB[a]

	gel before TTAB removal	
% surfactant	small-q peak [nm]	large-q peak [nm]
1.0	>13	ND[b]
2.0	>12	ND
2.5	11.9	ND
5.0	10.7	ND
10	10.1	ND
15	9.7	ND
20	10.4	ND
22	9.6	ND
25	10.3	4.1
28	10.9	4.1
30	ND	4.1
40	ND	4.0

[a] The data for 1−10% are shown in Figure 6, and the data for 10−40% are shown in Figure 7. [b] ND = not distinguishable.

Gels with high TTAB concentrations formed clear but became white while the surfactant soaked out. To quantify this, the transmitted intensity of a helium−neon laser was monitored as a function of soaking time for gels formed with several TTAB concentrations. Gels formed in the presence of up to 20% TTAB were transparent before and after soaking. Gels formed in the presence of 25% and 28% scattered light weakly. The transmittance was approximately 90% after polym-

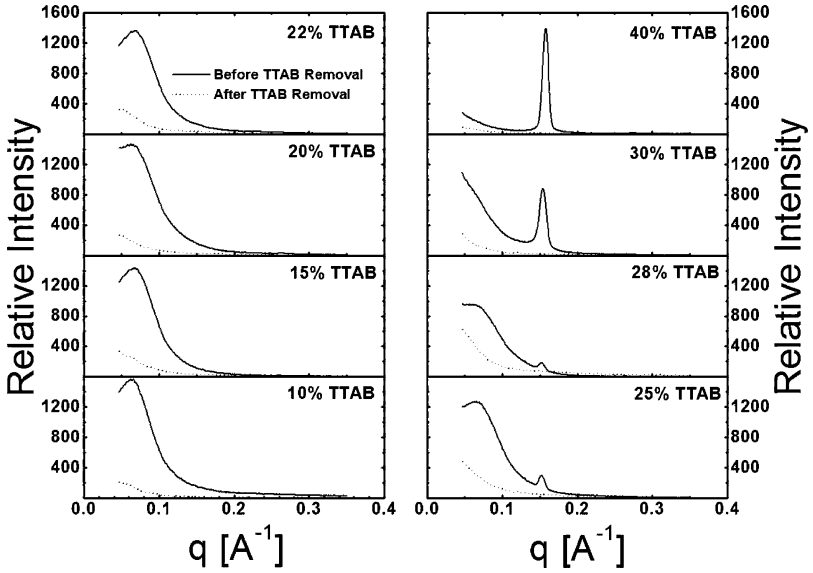

Figure 7. Upper curves are circularly averaged intensity plots for all data shown in Figure 5 prior to the removal of TTAB. Lower curves are $I(q)$ for gels that were formed in the presence of TTAB but then were soaked to remove it, crushed, and inserted in capillaries.

erization and increased slightly upon soaking. Before soaking gels formed in the presence 30% and 40% TTAB transmitted about 65% and 20% of the incident light, respectively. The transmission coefficient of the gel formed in the presence of 30% TTAB slowly declined and became close to zero after soaking for about 60 min, while the gel formed in the presence of 40% TTAB became opaque in about 5 min.

The cross-linker concentration is known to have a direct effect on the gel structure.[27] High concentrations of the cross-linker lead to the formation of clustered gels. Clustered gels scatter light significantly. Hence, the effect of the cross-linker concentration on the optical transmission of the gels formed in the presence of various concentrations of TTAB was studied. A set of stock solutions with varying cross-linker concentrations of 1.75%, 3.5%, 5.25%, and 7% were prepared. Gels were formed after the addition of different amounts of TTAB to these solutions and then soaked in water to remove the surfactants prior to optical transmission measurements. All the gels were optically transparent after polymerization, but before surfactant removal. Gels formed in the presence of 0−28% surfactant remained transparent irrespective of cross-linker concentration. All gels formed with 30% or more surfactant became uniformly white as the surfactants were removed.

Clear gels formed in the presence of high concentrations of TTAB become white when the surfactant is removed, independent of cross-linker concentration. The effect of soaking the gels in solutions of different concentrations of TTAB was studied. Two experiments were designed. In the first, all gels were soaked in distilled water to remove the surfactants completely. The gels were then cut into 1 cm × 1 cm pieces and soaked in solutions containing 10, 20, 30, or 40% TTAB for at least 10 days. The gels were removed, rinsed in distilled water, and viewed. The gels that initially remained clear stayed clear. The gels that turned opaque and white upon soaking in distilled water stayed white even after soaking in TTAB solutions. In the second experiment, gels were soaked in TTAB solutions without prior removal of surfactants. Gels formed in the presence of 30% and 40% TTAB still turned white when soaked in solutions containing ≤30% TTAB, but much more slowly than when soaked in water.

Time-separated photographs of a gel formed in the presence of 40% TTAB and then soaked in the solutions indicated are shown in Figure 8. The center flask in each image shows the white gel obtained on soaking in distilled water. The gel soaked in 30% TTAB solution was almost clear after 30 min and progressively became white. The gel soaked in 40% TTAB solution remained translucent throughout the experiment.

The white gels scatter light of all wavelengths strongly, indicating that there are fluctuations in the index of refraction on optical length scales. Apparently, as the TTAB diffused out, refractive index variations on optical length scales became more significant. Studies on the effect of drying on the optical transparency of the gels shed light on this hypothesis.

All the gels, including the ones that were opaque and white, shrank and became a hard, optically transparent material when dried in air. Gels regained their swollen state upon soaking in water, and the gels that were white before drying again became white after soaking in water.

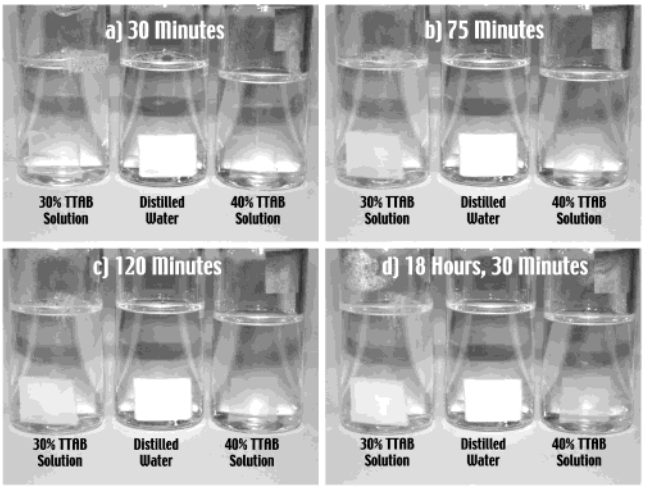

Figure 8. Time-separated photographs of three sample of the same gel formed in the presence of 40% TTAB and soaked in different solutions as indicated.

Table 4. Refractive Index Measurements for Different Concentrations of Acrylamide, TTAB in Buffer, and Pregel Solutions

% solute	acrylamide in buffer	TTAB in buffer	pregel solution
0[a]	1.3349	1.3349	1.4005
10	1.3506	1.3499	1.4066
20	1.3672	1.3651	1.4181
30	1.3836	1.3851	1.4273
40	1.4005	1.3987	1.4325

[a] The refractive index value for 0% acrylamide and TTAB in buffer are that of 1 × TBE buffer solution. The refractive index value for 0% pregel solution is that of 40% acrylamide solution.

Refractive index measurements of various concentrations of acrylamide in buffer, TTAB in buffer, and pregel solutions help to explain the transition from clear to white gels. These measurements are summarized in Table 4. The pregel solutions all have indices of refraction close to 1.41. Removal of TTAB after polymerization leaves regions in the gel that have an index of refraction of 1.33 (that of water). Calculations presented elsewhere[20] indicate that fluctuations in the index of refraction of that magnitude on several hundred nanometer length scales will appear white.

4. Discussion

The extensive family of experiments performed allows for a good understanding of the resulting gel structure when acrylamide is polymerized in the presence of TTAB. Key results include that (1) acrylamide drives the TTAB micellar to columnar transition to higher surfactant concentrations; (2) during polymerization, for the acrylamide solutions containing 30% and 40% TTAB, much of the TTAB is driven into nanodomains of columnar phase; (3) polyacrylamide gels formed in the presence of TTAB have a larger storage modulus than the same concentration polyacrylamide; and (4) intense small-angle X-ray scattering for polyacrylamide gels containing 10%−28% TTAB indicates a constant length scale separating micelles.

Polarized light microscopy, viscosity measurements, and X-ray scattering studies show that the micellar to hexagonal−columnar phase transition of TTAB occurs at about 10% higher concentration when acrylamide monomer is present in solution. For TTAB in buffer, a transition from an isotropic phase of micelles to hex-

agonal columnar phase occurred at about 35% surfactant. This was confirmed by characteristic signatures of the hexagonal phase such as birefringence, high viscosity, and anisotropic X-ray scattering. No birefringence was observed in any of the TTAB in acrylamide solutions up to 40% TTAB, and the viscosities of the TTAB in 40% buffered acrylamide solutions remained relatively low (<70 mPa s). The 40% TTAB in 40% buffered acrylamide solution showed isotropic X-ray scattering. When the TTAB concentration in 40% buffered acrylamide solution was increased to 45%, birefringence was observed accompanied by a substantial increase in viscosity (400 mPa s) (Figure 1). These results suggest that the presence of acrylamide does not prevent the formation of TTAB micelles, but it does shift the boundary for the isotropic micellar phase to the hexagonal columnar phase transition from about 35% to 45% TTAB.

Real-time dynamic viscosity measurements showed that TTAB profoundly affects the process of gelation. The dynamic viscosities ($|\eta^*|$) for the gels formed in the presence of 30% and 40% TTAB showed a gradual and substantial increase during the induction stage. The $|\eta^*|$ values just prior to the gel point were almost identical to the viscosities of 30% and 40% TTAB solutions in buffer, respectively (section 3.2). The increase in $|\eta^*|$ prior to gelation seen in Figure 3 for a few hundred seconds before the gel point for the 30% and 2500 s before for the 40% TTAB solutions is consistent with phase separation into polymer gel-rich and surfactant-rich mesophases.[12] When the acrylamide monomers start to polymerize in the presence of high TTAB concentrations, the surfactants phase separate, and regions rich in surfactant are formed. The high local concentrations of surfactant lead to the formation of columnar phase regions. This interpretation of the "pregel" dynamic viscosity is confirmed by X-ray diffraction of gels containing TTAB.

The X-ray diffraction measurements of polyacrylamide gels containing 30% and 40% TTAB (Figure 7) show large narrow peaks centered at $q = 0.155$ Å^{-1}, corresponding to the 4.1 nm separation of columns in the hexagonal phase. In addition, these samples were birefringent, indicative of the columnar hexagonal phase as well. Thus, we suggest that, in the process of gelation of the 30% and 40% TTAB in 40% acrylamide, growing polyacrylamide chains force TTAB to separate into nanodomains of columnar phase. The increase in $|\eta^*|$ prior to the gel point suggests that these nanodomains dominate the viscoelastic properties of the solution just before the gel point. Then, when the system gels, these nanodomains are trapped in place.

Figure 4 shows that the storage modulus increases with added TTAB concentration. Different amounts of TTAB surfactant were added to a 40% acrylamide stock solution. The final gel contains the reported concentrations of TTAB. Presuming the surfactant molecules become hydrated when they dissolve (which they must), there are fewer water molecules available surrounding the polyacrylamide chains. Thus, the effective local polyacrylamide concentration is higher in gels with more added TTAB. This combination apparently leads to higher stiffness.

X-ray scattering experiments show a strong signal at small angles. The peak of that scattering increases in q as TTAB concentration increases from 1% to 10% and then remains at approximately constant q from 10% to 28%. We can understand the increase in q for lower TTAB concentrations as micelles spaced closer together as the concentration increases.

Let d be the diameter of the spherical particle (micelle) and $V = (\pi/6)d^3$ its volume. If V_s is the volume available per particle, let us define $a_s = V_s^{1/3}$. The volume fraction ϕ is then given by

$$\phi = V/V_s \tag{3}$$

Substituting for V and V_s in terms of d and a_s, respectively

$$\frac{a_s}{d} = \left(\frac{\pi}{6}\frac{1}{\phi}\right)^{1/3} \tag{4}$$

For a given diameter of the particle and a known volume fraction, the distance between two adjacent particles can be calculated using eq 4.

Thus, since several measurements of micelle diameter are consistent with 4.1 nm, this model predicts a decrease of a_s from 15.3 to 4.5 nm for volume fractions of 0.010 to 0.40. Unfortunately, the smallest q for useable diffraction data was $q = 0.047$ Å^{-1}. The length scale associated with that q would be 13.4 nm. For volume fractions of 0.02, 0.025, 0.05 and 0.10, the predicted values of a_s are 12.2, 11.3, 9.0, and 7.1 nm, respectively. As seen in Table 3, the distances associated with the peaks of smallest q range from larger than 13 nm for volume fractions of 0.01 to essentially constant at 10 nm for volume fractions from 0.05 to 0.28. Thus, the data are consistent with an isotropic distribution of 4.1 nm diameter micelles separated by the distance predicted by packing considerations only to an average spacing of 10 nm (for a volume fraction between 0.025 and 0.05). For higher volume fractions the micelles apparently remain separated by, on average, 10 nm. In order for this to be the case, even with larger concentrations of TTAB, the TTAB not in an isotropic distribution of micelles must phase separate into surfactant-rich regions.

The appearance of a low-intensity scattering peak at $q = 0.153$ Å^{-1} corresponding to a 4.1 nm length scale in the gels formed in the presence of 25% and 28% TTAB concentration may be evidence of this phase separation. It was argued above that the sharp peaks centered at $q = 0.153$ Å^{-1} in the gels formed in the presence of 30% and 40% TTAB are due to formation of hexagonal−columnar phase nanodomains. For these higher concentrations the intensity scattered at smaller angles is less than for the lower concentrations. Thus, the nanodomain structure with characteristic size of hundreds of nanometers due to formation of columnar phase regions dominates for ≥30% TTAB gels, while micelles separated by at least 10 nm dominate the scattering for lower concentrations. After the removal of the surfactant, the peak corresponding to the micelle diameter of 4.1 nm disappears, and the small-angle scattering intensity is much less due to lack of contrast.[12,28]

A molecular level description can now be proposed. The data indicate that for added TTAB concentrations ≤28% polyacrylamide forms around TTAB micelles. The micelles are prevented from being closer than 10 nm on average. Thus, for 5−28% added TTAB, the polyacrylamide network has a minimum cross section of 6 nm. The mean pore radius of a 20% polyacrylamide network is 0.64 nm.[11] The 40% polyacrylamide network would be closer together. A hydrated polyacrylamide

chain has radius of about 0.3 nm; thus, the minimal cross-sectional distance of 6 nm will contain on the order of six cross-linked polyacrylamide chains. The cross-linker density is 7% of the acrylamide density, corresponding to one cross-linker per 26 acrylamide (bisacrylamide has a molecular mass about twice that of acrylamide). At 0.25 nm per acrylamide, there is expected to be a cross-link every 6 nm of contour length along each chain.

The model proposed for the gel structure here is also in agreement with the optical transmission observations. Optical clarity is an indication that the index of refraction does not vary on optical length scales. White materials either reflect all colors without absorption or, more commonly, scatter all colors well. When broken up, the pieces of white gel remained white. Thus, the whiteness was not because the surface alone was an excellent diffuse scatterer. The transformation of a gel from clear to white thus indicates that there was a significant change in light scattering throughout the gel as the surfactant diffused out.

As mentioned earlier, all the gels were optically transparent after polymerization but before surfactant removal. Gels formed in the presence of 30% or more surfactant became uniformly white as the surfactants were removed. Those formed with 0−28% surfactant remained transparent. The optical transmission changes observed as a function of the cross-linker concentration indicate that the structural changes associated with forming polyacrylamide gels in the presence of surfactant is independent of the cross-linker concentration. The study on the effect of drying on the optical clarity of the gels showed that all gels became transparent upon drying irrespective of surfactant concentration. The gels that were white when hydrated regained their opacity upon soaking in water. This clearly shows that the scattering is due to refractive index fluctuations.

The refractive index measurements of solutions (Table 4) and the observations of the change in optical transmission of gels on soaking (Figure 8) indicate that though there may be large domains of surfactant-rich regions in the gel matrix, the refractive indices of the polymer-rich region and the surfactant-rich region are well matched and their fluctuations are small. When the surfactant is removed and the large nanodomain regions are filled with water, there is a significant difference in the refractive index between the polyacrylamide and the water-rich regions. The large fluctuations in the refractive index between the polymer-rich region and aqueous regions make these gels scatter light strongly.

Prior work on the synthesis of polymer gels in the presence of lyotropic surfactant phases provides further support for the proposed model. Antonietti et al.[12,13,17] reported SEM images of replica structures of polymer gels that had been formed in the presence of various surfactants. Many of those images seem to show large irregular pores on many length scales, including hundreds of nanometers. The AFM observations reported in ref 19 further demonstrate that there is a dramatically different surface morphology for the gels that turned white compared with those that remained clear. Turbidity calculations based on a detailed scaling analysis of the AFM images of gel surfaces and refractive index fluctuations show an increase in the turbidity by about 6 orders of magnitude for the 0% surfactant gel to the 40% surfactant gel.[20] The results presented here are in agreement with these previously reported observations and the proposed model.

5. Conclusion

A comprehensive study of a very complex surfactant−gel system is reported. The presence of acrylamide monomer in solution was found to significantly alter the phase diagram of TTAB surfactant. In the process of polymerizing, the incipient gel network caused changes in the TTAB self-organization, resulting in formation of columnar phase nanodomains. A surprising limit of 10 nm in closest approach of micelles remaining within the final gels was discovered. The stiffness of gels after TTAB removal was found to increase with the concentration of added TTAB.

Polarized optical microscopy, viscosity measurements, and X-ray scattering studies of the pregel solutions clearly indicated a shift in the phase transition boundary of TTAB due to the presence of acrylamide. The acrylamide monomers do not prevent the formation of micelles, but the transition from an isotropic micellar phase to a hexagonal columnar phase occurs at a much higher concentration in the presence of acrylamide. This implies that higher volume of surfactants can be used to direct the formation of nanostructured hydrogels.

Real-time viscosity measurements provided useful insight into the initial stages of the polymerization reaction. No indication of phase separation of polymer and surfactant was observed in the gels formed in the presence of low TTAB concentrations. A demixing of the polymer and the surfactant phase occurred in the gels formed in the presence of high TTAB concentrations. X-ray scattering experiments showed that the bulk structure of the gels were dependent on the amount of TTAB present during polymerization. Formation of acrylamide gels in the presence of TTAB yielded extremely durable highly macroporous gels independent of the polymer or cross-linker concentration. A model based on symmetry and packing considerations for lattices of spheres of different concentrations was developed. This model was successfully used to interpret the physical observations and the experimental results.

Synthesizing polymer gels in the presence of surfactant self-assemblies thus provides a route for the design and synthesis of nanostructured hydrogels.

Acknowledgment. We thank P. A. Rikvold and A. Beheshti for useful discussions. T. Somasundaram and J. C. Billings are acknowledged for their assistance in the X-ray scattering experiments and rheology measurements, respectively. This research was supported by Florida State University through the Center for Materials Research and Technology (MARTECH) and the University's Graduate Fellow program.

References and Notes

(1) Patterson, B. C. Surfactant micelles as templates in hydrogels. Ph.D. Dissertation, Florida State University, Tallahassee, 2000.
(2) Barton, J.; Juranicova, V.; Vaskova, V. *Makromol. Chem.* **1985**, *186*, 1935.
(3) Vaskova, V.; Juranicova, V.; Barton, J. *Chem. Pap.* **1986**, *40*, 435.
(4) Righetti, P. G.; Caglio, S.; Saracchi, M.; Quaroni, S. *Electrophoresis* **1992**, *13*, 587.
(5) Laversanne, R. *Macromolecules* **1992**, *25*, 489.
(6) Vaskova, V.; Klimova, M.; Barton, J. *Angew. Makromol. Chem.* **1995**, *229*, 133.
(7) Chiari, M.; Righetti, P. G. *Electrophoresis* **1995**, *16*, 1815.

(8) Rill, R. L.; Locke, B. R.; Liu, Y.; Dharia, J.; Van Winkle, D. H. *Electrophoresis* **1996**, *17*, 1304.
(9) Charlionet, R.; Levasseur, L.; Malandain, J.-J. *Electrophoresis* **1996**, *17*, 58.
(10) Deriu, A.; Cavatorta, F.; Asnaghi, D.; Bossi, A.; Righetti, P. G. *Physica B* **1997**, *234*−*236*, 271.
(11) Rill, R. L.; Van Winkle, D. H.; Locke, B. R. *Anal. Chem.* **1998**, *70*, 2433.
(12) Antonietti, M.; Goltner, C.; Hentze, H.-P. *Langmuir* **1998**, *14*, 2670.
(13) Antonietti, M.; Caruso, R. A.; Goltner, C. G.; Weissenberger, M. C. *Macromolecules* **1999**, *32*, 1383.
(14) Zeng, X.; Qian, W.; Siqing, C.; Yuanqin, Z. *J. Dispersion Sci. Technol.* **1999**, *20*, 1263.
(15) Zeng, X.; Qian, W.; Siqing, C.; Yuanqin, Z. *J. Dispersion Sci. Technol.* **1999**, *20*, 1273.
(16) Zeng, X.; Chen, Y. *J. Dispersion Sci. Technol.* **2000**, *21*, 449.
(17) Antonietti, M.; Caruso, R. A.; Hentze, H.-P.; Goltner, C. *Macromol. Symp.* **2000**, *152*, 163.
(18) Paul, E. J.; Prud'homme, R. K. In *Reactions and Synthesis in Surfactant Systems*; Texter, J., Ed.; Surfactant Science Series Vol. 100; Marcel Dekker: New York, 2001.
(19) Chakrapani, M.; Van Winkle, D. H.; Patterson, B. C.; Rill, R. L. *Langmuir* **2002**, *18*, 6449.
(20) Chakrapani, M.; Mitchell, S. J.; Van Winkle, D. H.; Rikvold, P. A. *J. Colloid Interface Sci.* **2003**, *258*, 186.
(21) *Peakfitv4.0 for WindowsUser's Manual;* AISN Software Inc.: San Rafael, CA, 1995.
(22) Wärnheim, T.; Jönsson, A. *J. Colloid Interface Sci.* **1988**, *125*, 627.
(23) Itri, R.; Amaral, L. Q. *Phys. Rev. E* **1993**, *47*, 2551.
(24) Venable, R. L.; Nauman, R. V. *J. Phys. Chem.* **1964**, *68*, 3498.
(25) Norisuye, T.; Shibayama, M.; Nomura, S. *Polymer* **1998**, *39*, 2769.
(26) Winter, H. H.; Chambon, F. *J. Rheol.* **1986**, *30*, 367.
(27) Richards, E. G.; Temple, C. J. *Nature Phys. Sci.* **1971**, *230*, 92.
(28) Burban, J. H.; He, M.; Cussler, E. L. *AIChE J.* **1995**, *41*, 907.

MA034814M